Distinct roles for Pax7 and Pax3 in adult regenerative myogenesis

Shihuan Kuang,[1] Sophie B. Chargé,[1] Patrick Seale,[2] Michael Huh,[1,3] and Michael A. Rudnicki[1,2,3]

[1]Molecular Medicine Program, Ottawa Health Research Institute, Ottawa, Ontario, Canada K1H 8L6
[2]Department of Biology, McMaster University, Hamilton, Ontario, Canada L8S 4K1
[3]Department of Cellular and Molecular Medicine, University of Ottawa, Ottawa, Ontario, Canada K1H 8M5

We assessed viable *Pax7*$^{-/-}$ mice in 129Sv/J background and observed reduced growth and marked muscle wasting together with a complete absence of functional satellite cells. Acute injury resulted in an extreme deficit in muscle regeneration. However, a small number of regenerated myofibers were detected, suggesting the presence of residual myogenic cells in *Pax7*-deficient muscle. Rare Pax3^{+}/MyoD^{+} myoblasts were recovered from *Pax7*$^{-/-}$ muscle homogenates and cultures of myofiber bundles but not from single myofibers free of interstitial tissues. Finally, we identified Pax3^{+} cells in the muscle interstitial environment and demonstrated that they coexpressed MyoD during regeneration. Sublaminar satellite cells in hind limb muscle did not express detectable levels of Pax3 protein or messenger RNA. Therefore, we conclude that interstitial Pax3^{+} cells represent a novel myogenic population that is distinct from the sublaminar satellite cell lineage and that Pax7 is essential for the formation of functional myogenic progenitors from sublaminar satellite cells.

Introduction

Muscle satellite cells are thought to represent the only population of committed myogenic progenitors in adult skeletal muscle. The activation of muscle satellite cells generates proliferative myogenic precursor cells that differentiate to repair and replace damaged fibers (Charge and Rudnicki, 2004). The transcription factors regulating the specification and differentiation of satellite cell–derived myogenic progenitors is analogous to the molecular mechanisms regulating embryonic myogenesis (Parker et al., 2003). Pax7, a paired-box transcription factor, is specifically expressed in quiescent and newly activated satellite cells. Importantly, the absence of myogenic cells in young *Pax7*$^{-/-}$ skeletal muscle demonstrates a requirement for Pax7 in the function of the satellite cell lineage (Seale et al., 2000). *Pax7*$^{-/-}$ mice appear normal at birth but fail to thrive and subsequently die at 2–3 wk from unknown causes (Mansouri et al., 1996; Seale et al., 2000). The decreased caliber of *Pax7*$^{-/-}$ myofibers is attributable to the lack of satellite cell fusion during the postnatal growth of muscle (Seale et al., 2000). However, the normal appearance of newborn *Pax7*$^{-/-}$ muscle suggests that embryonic and fetal myogenesis is unaffected and identifies a unique requirement for Pax7 in the satellite cell lineage.

Recent work has identified stem cell populations capable of giving rise to satellite cells during regeneration. Muscle-derived side-population cells separated on the basis of Hoechst dye exclusion give rise to satellite cells after intramuscular or intravenous injection (Gussoni et al., 1999; Asakura et al., 2002). In addition, bone marrow–derived cells similarly have the capacity to engraft skeletal muscle and form myogenic satellite cells after whole-body irradiation and transplantation (Ferrari et al., 1998; Bittner et al., 1999; Gussoni et al., 1999; LaBarge and Blau, 2002). More recently, we demonstrated that endogenous CD45^{+} muscle-derived cells give rise to Pax7^{+} myogenic cells in response to Wnt proteins during regeneration (Polesskaya et al., 2003). Furthermore, ectopic expression of Pax7 in CD45^{+}/Sca1^{+} cells is sufficient for their myogenic specification (Seale et al., 2004). Together, these data support the notion that a developmental relationship exists between adult stem cells and Pax7-dependent satellite cell myogenic lineages.

Pax3, a paralogue of Pax7, is critical for the delamination and migration of the somitic muscle progenitor cells to the limb buds, as *Pax3* mutant mice lack limb muscles (Bober et al., 1994; Goulding et al., 1994; Tajbakhsh et al., 1997). Despite these distinct functions of Pax3 and -7 in muscle development (Relaix et al., 2004), recent studies have begun to elucidate a

S. Kuang and S.B. Chargé contributed equally to this paper.

Correspondence to Michael A. Rudnicki: mrudnicki@ohri.ca

P. Seale's present address is Dana-Farber Cancer Institute, Boston, MA 02115.

Abbreviations used in this paper: β-gal, β-galactosidase; CTX, cardiotoxin; EDL, extensor digitorum longus; MyHC, myosin heavy chain; P, postnatal day; TA, tibialis anterior.

The online version of this article contains supplemental material.

The Journal of Cell Biology, Vol. 172, No. 1, January 2, 2006 103–113
http://www.jcb.org/cgi/doi/10.1083/jcb.200508001

common playground for these paralogues. Specifically, a novel population of Pax3/Pax7 double-positive ($Pax3^+/Pax7^+$) stem cells were identified in the dermomyotome of the embryonic somites (Ben-Yair and Kalcheim, 2005; Gros et al., 2005; Kassar-Duchossoy et al., 2005; Relaix et al., 2005). Proliferating $Pax3^+/Pax7^+$ cells were observed to persist throughout embryonic and fetal development and later to give rise to a subset of muscle satellite cells. In the absence of muscle environment or Pax3/Pax7 expression, these somitic stem cells apoptose or adopt alternative nonmuscle lineages. Interestingly, Pax3 expression in satellite cells is mostly down-regulated before birth, although a subset of satellite cells appears to express Pax3 (Kassar-Duchossoy et al., 2005; Montarras et al., 2005; Relaix et al., 2005).

In this study, we set out to determine the relative role of Pax7 and -3 in postnatal muscle growth and regeneration. The original $Pax7^{-/-}$ mice in C57/B6 background appear normal at birth but fail to thrive and subsequently die at 2–3 wk of age (Mansouri et al., 1996; Seale et al., 2000), preventing them from further postnatal analysis. Therefore, *Pax7* carrying a knockin of a β-galactosidase (β-gal) cassette ($Pax7^{lacZ/lacZ}$) were backcrossed nine generations into the 129Sv/J genetic background, where some mutant mice were viable. These $Pax7^{lacZ/lacZ}$ 129Sv/J mice allow us to examine not only muscle growth and regeneration in the absence of Pax7 expression but also the function of Pax3 independent of Pax7 in postnatal muscles. We found that the growth and regeneration of $Pax7^{lacZ/lacZ}$ muscle was greatly compromised, suggesting an essential role for Pax7 in these processes. Furthermore, we identified a novel population of Pax3-expressing myogenic progenitors in the interstitial space of adult skeletal muscles. Together, these results demonstrate an essential role for Pax7 in the productive formation of myogenic progenitors during postnatal growth and regeneration of skeletal muscle.

Results

Decreased fiber size but not fiber number characterizes the decreased muscle growth in $Pax7^{lacZ/lacZ}$ mice

To investigate the role of Pax7 in postnatal muscle development, we examined the growth of $Pax7^{lacZ/lacZ}$ muscles during the postnatal period in the 129Sv/J genetic background. Growth of $Pax7^{lacZ/lacZ}$ mice appeared normal during embryonic development until birth, as demonstrated by the normal body weight as compared with control littermates at postnatal day (P) 0 (Table I). However, after birth, $Pax7^{lacZ/lacZ}$ mice failed to maintain normal postnatal growth. At P3, $Pax7^{lacZ/lacZ}$ mice were only two thirds of the weight of wild-type littermates, and at P10, they were less than half the weight of wild-type littermates. No significant weight difference was detected between $Pax7^{+/lacZ}$ and wild-type littermates (Table I). The decreased body mass of $Pax7^{lacZ/lacZ}$ mice was at least partially attributable to decreased skeletal muscle growth as revealed by the significant size/weight decreases in tibialis anterior (TA) and other skeletal muscles (Table I; unpublished data). To further determine whether the decreased muscle mass in $Pax7^{lacZ/lacZ}$ mice resulted from reduced myofiber size or number or both, we enumerated the total number of myofibers at muscle mid-belly and determined the myofiber cross-sectional area. The total fiber number in both extensor digitorum longus (EDL) and soleus muscles was not different between $Pax7^{lacZ/lacZ}$ and wild-type littermates at P10 (Table I). In contrast, myofiber size, regardless of their myosin heavy chain (MyHC) phenotypes, was found to be significantly decreased in $Pax7^{lacZ/lacZ}$ mice. More precisely, the cross-sectional areas of Types II and I myofibers (253 ± 16 and 289 ± 15 μm^2, $n = 4$, respectively) in the mutant soleus were ~1.5- and 1.8-fold smaller than those of wild-type fibers (374 ± 25 and 512 ± 29 μm^2, $n = 4$, respectively) at P10, whereas no significant difference in the cross-sectional area of Type I myofiber was detected at P0 ($Pax7^{lacZ/lacZ}$: 205 ± 37 μm^2, $n = 2$; $Pax7^{+/+}$: 192 ± 29 μm^2, $n = 2$). Together, these results suggest that the smaller fiber size found in $Pax7^{lacZ/lacZ}$ mice directly resulted from defects in postnatal growth. Furthermore, the myonuclei number per myofiber was significantly reduced to ~50% of the normal amount in adult $Pax7^{lacZ/lacZ}$ mice in both soleus and EDL muscles (Table I), suggesting a deficiency in (or lack of) satellite cell function to supply myonuclei to the growing myofibers. Altogether, these data demonstrate that postnatal growth of $Pax7^{lacZ/lacZ}$ skeletal muscles is severely retarded because of inadequate myonuclei increase and myofiber growth.

Muscle atrophy and fiber loss in aged $Pax7^{lacZ/lacZ}$ mice

To investigate the maintenance of $Pax7^{lacZ/lacZ}$ muscle during aging, we analyzed the muscle phenotype of aging mice. By 6 mo of age, $Pax7^{lacZ/lacZ}$ mice displayed prominent kyphosis (curvature of the spinal column), which is typical of extensive muscle wasting and a hallmark of aging (Fig. 1, A and B; Megeney et

Table I. **Decreases in muscle mass but normal fiber number in $Pax7^{lacZ/lacZ}$ muscle**

	Body mass (g)			TA mass (mg)	EDL fiber number	Soleus fiber number	EDL nuclei/fiber	Soleus nuclei/fiber
	P0	P3	P10	P10	P10	P10	P100	P100
$Pax7^{+/+}$	1.3 ± 0.05 ($n = 9$)	3.1 ± 0.1 ($n = 11$)	7.1 ± 0.3 ($n = 11$)	5.6 ± 0.6 ($n = 8$)	947 ± 40 ($n = 5$)	897 ± 107 ($n = 3$)	ND	ND
$Pax7^{+/lacZ}$	1.2 ± 0.04 ($n = 10$)	3.0 ± 0.1 ($n = 15$)	6.8 ± 0.3 ($n = 13$)	5.4 ± 0.3 ($n = 10$)	ND	ND	227 ± 5 ($n = 20$)	402 ± 8 ($n = 20$)
$Pax7^{lacZ/lacZ}$	1.3 ± 0.05 ($n = 5$)	1.9 ± 0.1[a] ($n = 9$)	3.0 ± 0.3[a] ($n = 8$)	1.6 ± 0.3[a] ($n = 6$)	1,028 ± 61 ($n = 5$)	865 ± 250 ($n = 3$)	142 ± 6[a] ($n = 20$)	170 ± 8[a] ($n = 10$)

[a]Significant at $P < 0.01$.

al., 1996). Evidence for muscle wasting was strikingly depicted by a progressive decline in the number of TA myofibers from 2–3 mo of age (Fig. 1 C). At 6–7 mo, the number of TA fibers in *Pax7*$^{lacZ/lacZ}$ mice was decreased to one third of that in *Pax7*$^{+/+}$ muscle (Fig. 1 C). The decreased myofiber number was attributable to a specific loss of fast IIb fibers as demonstrated by TA fiber–type analysis (not depicted) and by the normal fiber number found in the slow soleus muscle of adult *Pax7*$^{lacZ/lacZ}$ mice (Fig. 1 D). Despite the massive fiber loss in adult *Pax7*$^{lacZ/lacZ}$ TA, the number of newly regenerated myofibers, as indicated by the centrally located nuclei (5 ± 1 per cross section, $n = 8$), remained comparable to that of wild-type littermates (4 ± 1, $n = 7$). Therefore, these observations suggest that an impaired regeneration process is failing to replace the rapid loss of fast myofibers associated with aging in *Pax7*$^{lacZ/lacZ}$ mice. The presence of calcium deposits in adult *Pax7*$^{lacZ/lacZ}$ TA muscles further demonstrated the defective regenerative response during aging (Fig. 1, E and F). Finally, *Pax7*$^{lacZ/lacZ}$ muscle fibers did not display signs of extensive damage, suggesting that the loss of muscle did not result in a reduction in fiber integrity. Specifically, *Pax7*$^{lacZ/lacZ}$ fibers were resistant to Evans blue dye incorporation (unpublished data), and serum creatine kinase levels were normal at all ages studied (216 ± 92 U/liter [$n = 2$] and 579 ± 179 U/liter [$n = 6$] in *Pax7*$^{lacZ/lacZ}$; 328 ± 206 U/liter [$n = 2$] and 1148 ± 500 U/liter [$n = 6$] in *Pax7*$^{+/+}$ at P3 and in adults, respectively). Together, these results demonstrate that muscle wasting accompanied by a specific loss of fast fibers in *Pax7*$^{lacZ/lacZ}$ mice is accelerated as a function of age, and the accelerated fiber loss is not adequately compensated because of an impairment in muscle regenerative ability.

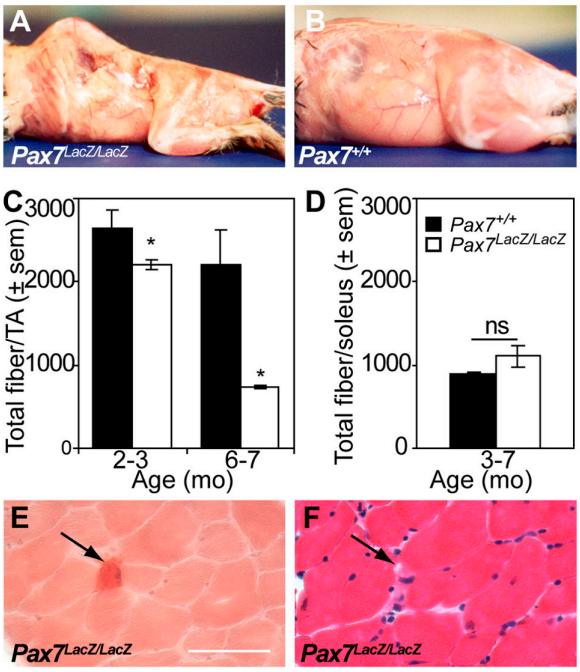

Figure 1. **Accelerated muscle wasting in adult *Pax7*$^{lacZ/lacZ}$ mice.** (A and B) By 6 mo of age, *Pax7*$^{lacZ/lacZ}$ (A) mice develop a curvature of the spine characteristic of extensive muscle wasting compared with wild-type littermates (B). (C) Total fiber number per TA is significantly reduced in *Pax7*$^{lacZ/lacZ}$ mice compared with wild-type littermates ($n = 4$ and 5 for 2–4 mo and $n = 2$ and 2 for 6–7 mo for *Pax7*$^{+/+}$ and *Pax7*$^{lacZ/lacZ}$, respectively). *, $P < 0.05$. (D) Total fiber number per soleus is not affected in *Pax7*$^{lacZ/lacZ}$ mice compared with wild-type littermates ($n = 2$ for each genotype). (E and F) Small calcium deposits (arrows) stained with Alizarin red (E) are present in between *Pax7*$^{lacZ/lacZ}$ myofibers, which otherwise appear normal, albeit smaller, on a spaced serial cross section stained with hematoxylin–eosin (F).

Severely deficient regeneration of *Pax7*$^{lacZ/lacZ}$ muscle after acute injury

To assess the regenerative capacity of *Pax7*$^{lacZ/lacZ}$ muscle, we injected cardiotoxin (CTX) into TA muscles to chemically induce injury. At 10 d and 1 mo after CTX injection, *Pax7*$^{+/+}$ TA regained the overall normal appearance of regenerated muscle characterized by numerous centrally nucleated regenerating myofibers (Fig. 2, A and B). There were >700 regenerating fibers per TA cross section at both 10 d ($n = 2$) and 1 mo ($n = 3$) after injury, without appreciable deposition of calcium, adipose, or fibrotic tissues (Fig. 2, A–D). In sharp contrast, *Pax7*$^{lacZ/lacZ}$ TA displayed a severe regeneration deficit, with only rare centrally nucleated myofibers observed at 10 d (9 ± 6 fibers/TA cross section, $n = 3$) and 1 mo (61 ± 50 fibers/TA cross section, $n = 4$) after injection (Fig. 2, E and F). The centrally nucleated myofibers in *Pax7*$^{lacZ/lacZ}$ TA failed to mature and remained significantly smaller than those in *Pax7*$^{+/+}$ controls even 1 mo after injury (compare Fig. 2 B with Fig. 2 F [arrows]). Furthermore, by 1 mo after injury, *Pax7*$^{lacZ/lacZ}$ TA had been replaced by extensive adipose tissue (Fig. 2 F, arrowheads), fibrotic tissue (Fig. 2 G, arrowhead), and deposition of calcium (Fig. 2 H). Similar results were obtained after CTX injection in gastrocnemius muscles (unpublished data). This almost complete absence of muscle repair in adult *Pax7*$^{lacZ/lacZ}$ mice appears to be the most striking regeneration deficit reported in any mouse model.

Muscle regeneration was also analyzed in *Pax7*$^{lacZ/lacZ}$ mice after physically (crush) induced injuries. Similar to CTX-induced muscle regeneration, *Pax7*$^{lacZ/lacZ}$ TA and gastrocnemius muscles (Fig. 2 K, arrows, and not depicted) contained only rare centrally nucleated myofibers with extensive calcium deposition (Fig. 2 L) and fibrosis (not depicted) 10 d after crush. In contrast, muscles from *Pax7*$^{+/+}$ littermates were fully regenerated with large centrally nucleated fibers (Fig. 2 I and not depicted) and without calcium deposits (Fig. 2 J). Together, these experiments indicate that Pax7 is necessary for efficient muscle regeneration.

The presence of small numbers of centrally nucleated myofibers in *Pax7*$^{lacZ/lacZ}$ muscle at 10 d and 1 mo after injury did, however, suggest a limited capacity for muscle differentiation. As in wild-type mice, the centrally nucleated fibers in *Pax7*$^{lacZ/lacZ}$ mutant expressed embryonic MyHC and high levels of Desmin (Fig. 2, O and P), confirming their newly regenerated state. In addition, regenerated fibers in both *Pax7*$^{+/+}$ and *Pax7*$^{lacZ/lacZ}$ muscles contained BrdU-labeled nuclei at 10 d after injury, indicating that proliferating cells had differentiated and fused into these myofibers (Fig. 2, M and N). Consistent with the regenerative deficit of *Pax7*$^{lacZ/lacZ}$ muscle, only 3.5% of BrdU-labeled nuclei were found within muscle fibers, compared with 45% of BrdU-positive nuclei within myofibers in

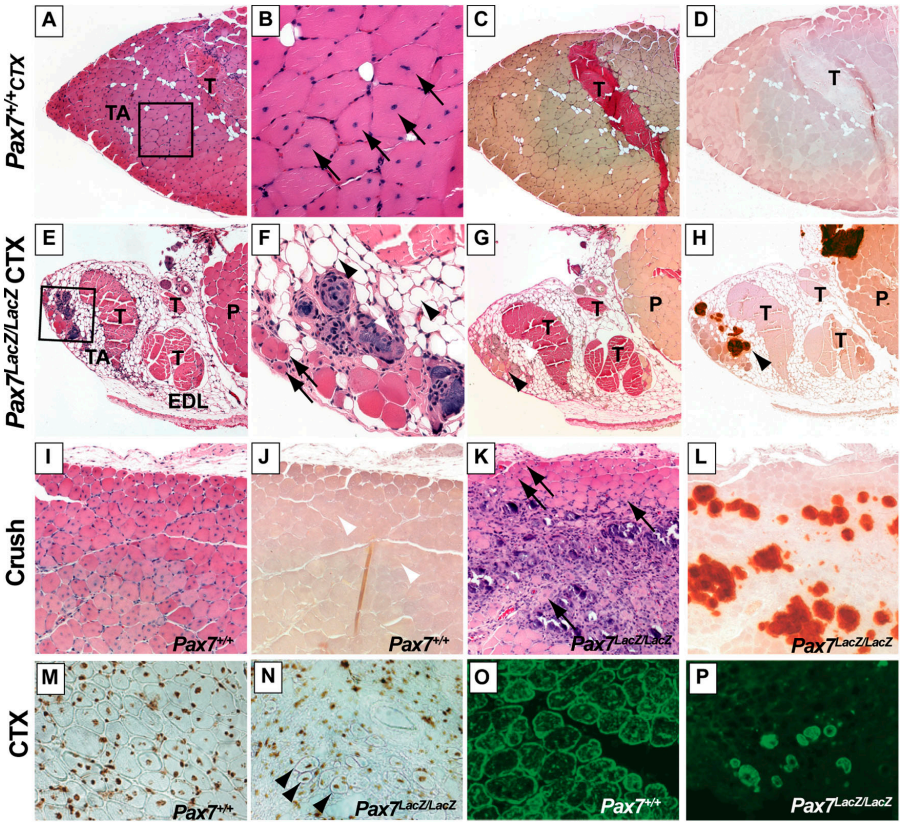

Figure 2. **Profound regeneration deficit in *Pax7*$^{lacZ/lacZ}$ muscle after acute injury.** Lower hind limb sections from *Pax7*$^{+/+}$ (A–D) or *Pax7*$^{lacZ/lacZ}$ (E–H) mice 1 mo after CTX stained with hematoxylin–eosin (A, B, E, and F), Van Gieson's (C and G; pink stain), and Alizarin red (D and H; red stain). (B and F) Higher magnifications of A and E, respectively. Note the efficient muscle regeneration in *Pax7*$^{+/+}$ TA characterized by numerous large centrally nucleated regenerating myofibers (B, arrows), with no extensive calcium deposition, adipogenesis, or fibrogenesis (A–D). In contrast, injured *Pax7*$^{lacZ/lacZ}$ TA (E–H) displays only rare and small centrally nucleated myofibers (F, arrows); instead, the muscle was replaced by calcium deposits (H, arrowhead), adipocytes (F, arrowheads), or fibrosis (G, arrowhead). Sections from *Pax7*$^{+/+}$ (I and J) and *Pax7*$^{lacZ/lacZ}$ littermates (K and L) 10 d after crush injury reveal an efficient muscle regeneration process in *Pax7*$^{+/+}$ TA (I), whereas only rare centrally nucleated myofibers are observed in *Pax7*$^{lacZ/lacZ}$ TA (K, arrows). Instead, muscle is infiltrated by inflammatory cells and replaced by fibrosis and large calcium deposits (L). The arrowheads in J indicate normal regenerative fibers in wild type. Central myonuclei in regenerated TA myofibers from *Pax7*$^{+/+}$ (M) and *Pax7*$^{lacZ/lacZ}$ (N) muscle 10 d after CTX injection are BrdU^{+} (DAB, brown; N, arrowheads) after multiple BrdU injections during the period of regeneration. Low efficiency of muscle regeneration in the *Pax7*$^{lacZ/lacZ}$ (P) is contrasted with the robust regeneration in *Pax7*$^{+/+}$ (O), as demonstrated by the expression of Desmin (FITC, green). P, plantarus; T, tendon.

regenerated *Pax7*$^{+/+}$ muscles. Finally, analysis of spaced serial cross sections demonstrated that regenerated *Pax7*$^{lacZ/lacZ}$ myofibers were multinucleated and extended over several hundred micrometers (unpublished data). Thus, by these criteria, the centrally nucleated *Pax7*$^{lacZ/lacZ}$ myofibers observed after muscle injury were regenerated rather than surviving myofibers.

Absence of functional satellite cells in *Pax7*$^{lacZ/lacZ}$ adult muscle

It has been reported that satellite cells are formed in the absence of Pax7 and that these cells have some capacity for myogenic function (Oustanina et al., 2004). Therefore, we examined whether we could similarly detect *Pax7*$^{lacZ/lacZ}$ satellite cells and whether these cells were capable of following the myogenic developmental program. First, we asked whether cells derived from Pax7 lineage, as marked by the expression of β-gal (see Materials and methods), were present on single muscle fibers in *Pax7*$^{lacZ/lacZ}$ mice. In *Pax7*$^{+/lacZ}$ mice, all β-gal^{+} cells also coexpressed Pax7 (Fig. 3 A) and vice versa, validating the absolute specificity of β-gal labeling. Rare β-gal^{+} cells were detected on EDL fibers isolated from younger (P25) *Pax7*$^{lacZ/lacZ}$ mice (Fig. 3 B). Although the Pax7^{+}/β-gal^{+} cells on *Pax7*$^{+/lacZ}$ myofibers typically displayed a small round shape indicative of activation by the single fiber isolation procedure, most *Pax7*$^{lacZ/lacZ}$ β-gal^{+} cells displayed a morphology characterized by a large cell body with long filopodium-like processes (Fig. 3, A and B). Furthermore, the frequency of β-gal^{+} cells on *Pax7*$^{lacZ/lacZ}$ mutant fibers (1.1 ± 0.2/fiber, $n = 28$) was ∼7% of that of the *Pax7*$^{+/lacZ}$ control (15.9 ± 2.2/fiber, $n = 25$) at P25. Even at birth (P0), the frequency of β-gal^{+} cells in the *Pax7*$^{lacZ/lacZ}$ mutant muscle (6.9 ± 1.3/microscopic field under 20×, $n = 7$) was less than half that of the *Pax7*$^{+/lacZ}$ control (16.0 ± 3.8/field, $n = 5$; Fig. S1, available at http://www.jcb.org/cgi/content/full/jcb.200508001/DC1). To examine whether the *Pax7*$^{lacZ/lacZ}$ β-gal^{+} cells were capable of proliferation upon activation, single fibers were isolated and cultured in horse serum–coated Petri dishes to prevent attachment of fibers. After 6 d of suspension culture, floating *Pax7*$^{+/lacZ}$ myofibers displayed characteristic large aggregates of proliferative satellite cell–derived myoblasts that expressed MyoD and/or Pax7 (Fig. 3, C and E). Under similar culture conditions, no aggregates of cells were found on *Pax7*$^{lacZ/lacZ}$ fibers ($n = 29$). Occasionally, pairs of nuclei that expressed low levels of MyoD were found within arrested single-blobbing cell bodies (Fig. 3, D and F). We did not detect Caspase3 expression in these cells (unpublished data), suggesting that Pax7 mutant satellite cells underwent an abortive mitosis and failed to complete cell division.

We next examined whether the Pax7-remnant cells on isolated single myofibers still retained typical satellite cell features. All satellite cells associated with freshly isolated *Pax7*$^{+/+}$ or *Pax7*$^{+/lacZ}$ fibers coexpressed Pax7 and Syndecan4 (Fig. 4, A and B) or CD34 (Fig. 4 H), suggesting that Syndecan4 (Cornelison et al., 2001) and CD34 (Beauchamp et al., 2000) are reliable markers of satellite cells. Specifically, 8.7 ± 1.9 Syndecan4^{+} cells/fiber and 3.9 ± 1.8 CD34^{+} cells/fiber were

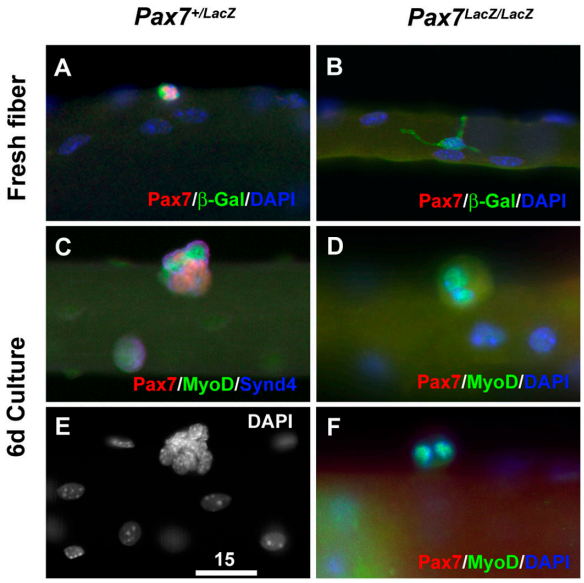

Figure 3. **Remnant nonfunctional β-gal$^+$ cells associated with muscle fibers in Pax7 mutant mice.** Expression of β-gal, knocked into the first coding exon of *Pax7* gene to generate the *Pax7* knockouts, in *Pax7*$^{+/lacZ}$ (A) and *Pax7*$^{lacZ/lacZ}$ (B) muscle fibers isolated from 1-mo-old mice. In *Pax7*$^{+/lacZ}$ muscle fibers, expression of β-gal is always colocalized with Pax7 expression. In *Pax7*$^{lacZ/lacZ}$ fibers, the β-gal$^+$ cells display large cell bodies and extensive filopodia-like processes (B), which are in contrast to the smaller, round morphologies of the β-gal$^+$ cells in the *Pax7*$^{+/lacZ}$ fibers (A). (C–F) After 6 d of suspended culture of single muscle fibers from *Pax7*$^{+/lacZ}$ mice, the Pax7$^+$ cells proliferate and differentiate to form aggregates of cells that express Pax7, MyoD, or both (C and E). Under identical culture conditions, the β-gal$^+$ cells associated with muscle fibers of *Pax7*$^{lacZ/lacZ}$ mice are unable to proliferate or differentiate (D and F). Bar, 15 μm.

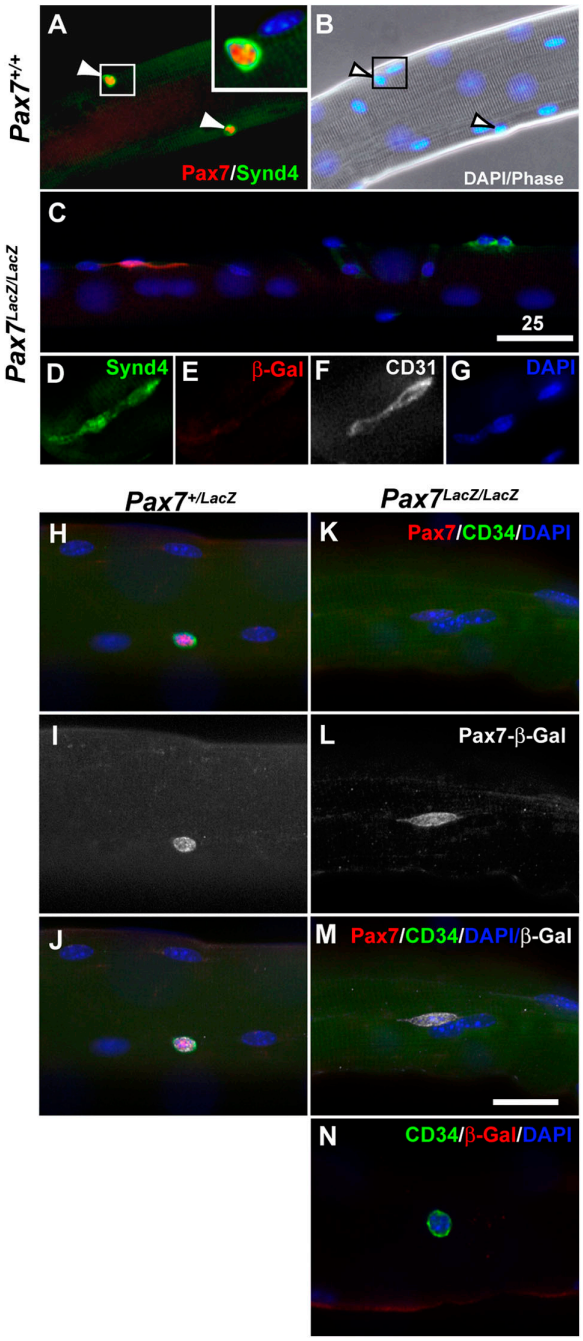

Figure 4. **Absence of satellite cell marker expression associated with adult *Pax7*$^{lacZ/lacZ}$ muscle fibers.** (A and B) Pax7 and Syndecan4 are coexpressed in satellite cells on freshly isolated *Pax7*$^{+/+}$ EDL fibers. Arrowheads show satellite cells and corresponding nuclei stained with DAPI. (C) In the *Pax7*$^{lacZ/lacZ}$ myofibers, few β-gal$^+$ cells (red) were identified, but they did not express the satellite cell marker Syndecan4 (green). (C–G) Conversely, the low frequencies of Syndecan4$^+$ cells associated with *Pax7*$^{lacZ/lacZ}$ myofibers were negative for β-gal but positive for the endothelial cells marker CD31. (H–J) Similarly, Pax7$^+$ and β-gal$^+$ cells on the *Pax7*$^{+/lacZ}$ myofibers are also positive for another satellite cell marker, CD34. (K–N) In the *Pax7*$^{lacZ/lacZ}$ myofibers, however, rare β-gal$^+$ and CD34$^+$ cells were never colocalized: the β-gal$^+$ cells were negative for CD34, and the CD34$^+$ cells were negative for β-gal. Bars, 25 μm.

detected in 6–8-wk-old adult *Pax7*$^{+/+}$ fibers (n = 16 fibers/3 mice for Syndecan4; n = 35 fibers/2 mice for CD34). In contrast, syndecan4 or CD34-expressing cells were never found on clean capillary-free *Pax7*$^{lacZ/lacZ}$ fibers (n = 56 fibers/3 mice for Syndecan4; n = 65 fibers/2 mice for CD34). Importantly, all β-gal–expressing cells on *Pax7*$^{lacZ/lacZ}$ fibers were negative for syndecan4 (Fig. 4 C) and CD34 (Fig. 4, K–M). However, occasionally syndecan4$^+$ or CD34$^+$ cells were found on *Pax7*$^{lacZ/lacZ}$ fibers when care was deliberately not taken during single fiber preparation. These cells were uniformly negative for β-gal immunostaining (Fig. 4, C–E and N). Notably, these syndecan4$^+$, β-gal$^-$ cells were also positive for the endothelial marker CD31 (Fig. 4, D–G). Together, these data demonstrate that although rare β-gal$^+$ cells are localized to the satellite cell niche in young *Pax7*$^{lacZ/lacZ}$ musculature, these cells have lost the characteristics and function of wild-type satellite cells.

In support of these findings, only 9% of *Pax7*$^{lacZ/lacZ}$ fiber (n = 76 fibers/3 mice) yielded any mononuclear cells (mean of 1.85 ± 0.34 cells/fiber) after several days of attached culture in growth medium. Importantly, the mononuclear cells associated with *Pax7*$^{lacZ/lacZ}$ fibers were uniformly negative for the myoblast-specific markers MyoD, Myf5, and Desmin (unpublished data). In contrast, all *Pax7*$^{+/+}$ fibers (n = 60 fibers/3 mice) gave rise to an average of 11.8 ± 0.97 cells/fiber. Furthermore, numerous proliferative bursts of *MyoD*$^+$ myoblasts were generated by all *Pax7*$^{+/+}$ fibers (unpublished data). Together, these data indicate that the defects in postnatal muscle growth and regeneration are attributable to an absence of functional satellite cells in *Pax7*$^{lacZ/lacZ}$ mutant mice.

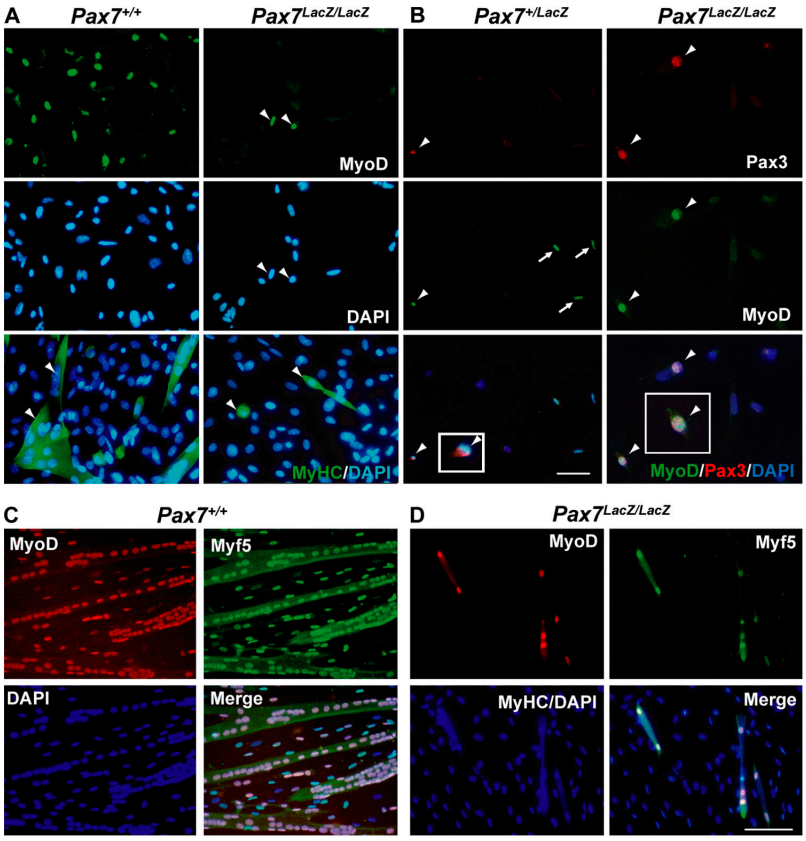

Figure 5. **Identification of Pax7-independent myogenic cells expressing Pax3.** (A, top and middle) Cell suspensions from *Pax7*$^{+/+}$ hind limb muscles grown in growth media for 15 h yielded large numbers of MyoD^{+} cells (FITC) compared with rare MyoD^{+} cells (arrowheads) observed in *Pax7*$^{lacZ/lacZ}$ preparations. (bottom) Myogenic cells obtained from both *Pax7*$^{+/+}$ and *Pax7*$^{lacZ/lacZ}$ hind limb muscles were capable of terminal differentiation as shown by MyHC expression (green; arrowheads) and fusion following 3 d in differentiation media. (B) Double immunostaining for Pax3 (red) and MyoD (green) of cell suspensions from *Pax7*$^{+/lacZ}$ or *Pax7*$^{lacZ/lacZ}$ limb muscle revealed that Pax3 and MyoD were coexpressed in certain myogenic cells (arrowheads). Cells expressing MyoD but not Pax3 were also detected in *Pax7*$^{+/+}$ and *Pax7*$^{lacZ/lacZ}$ cultures (arrows; not depicted). Insets show enlargements of the cells to the left. (C and D) Myogenic cells derived from cultures myofiber bundles of *Pax7*$^{+/+}$ (C) and *Pax7*$^{lacZ/lacZ}$ (D) mice. Myofiber bundle (20–30 fibers) were plated in a Matrigel-coated dish and culture in growth medium for 3 d followed by 1 d in differentiation medium. The green signals in the merged panels are intensified to help visualize myotubes. Bars, 12.5 μm.

Isolation of myogenic cells from *Pax7*$^{lacZ/lacZ}$ musculature

To identify the myogenic cells responsible for the small regenerative capacity in *Pax7*$^{lacZ/lacZ}$ hind limb muscle, single-cell suspensions were prepared from hind limb muscles and analyzed after 15 h in growth conditions or after an additional 3 d in differentiation medium. Interestingly, freshly isolated cell preparations from hind limb and diaphragm *Pax7*$^{lacZ/lacZ}$ muscles yielded some myogenic cells expressing MyoD (Fig. 5, A and B) or Myf5 (Fig. 5 D). Although present, *Pax7*$^{lacZ/lacZ}$ myogenic cells were recovered at an extremely low frequency (~1/150; Fig. 5) compared with wild-type muscle (363,012 ± 34,247 [n = 2] and 2,961 ± 1,096 [n = 4] MyoD^{+} cells and 242,132 ± 5,843 [n = 2] and 1,277 ± 578 [n = 3] Myf5^{+} cells/g of hind limb muscle for *Pax7*$^{+/+}$ and *Pax7*$^{lacZ/lacZ}$, respectively). The frequency of MyoD^{+} cells was not increased in cultures prepared from regenerating *Pax7*$^{lacZ/lacZ}$ TA 3–4 d after CTX injection (unpublished data).

At clonal density, *Pax7*$^{lacZ/lacZ}$ cells isolated from limb muscle formed small colonies of 6–20 MyoD^{+} and Desmin^{+} myoblasts after 10–20 d compared with proliferative bursts of >500 myoblasts in *Pax7*$^{+/+}$ cultures (unpublished data). The inability for *Pax7*$^{lacZ/lacZ}$ cells to expand in culture suggested a profound proliferative deficit under standard myoblast growth conditions as compared with myoblasts isolated from wild-type littermates. Even when cultured in the presence of high concentrations of growth factors (5% chick embryo extract; 50 ng/ml of stem cell growth factor; 1 μg/ml of insulin; Methocult M3434 [StemCell Technologies, Inc.] or in Matrigel-coated dishes), *Pax7*$^{lacZ/lacZ}$ myogenic cells did not proliferate. Nevertheless, *Pax7*$^{lacZ/lacZ}$ myogenic cells underwent myogenic differentiation and expressed MyHC after culture in low-mitogen medium after 3–5 d (Fig. 5 A). In myoblast preparations from *Pax7*$^{+/+}$ or *Pax7*$^{+/lacZ}$ muscles, an average of 311.3 ± 49.3 (n = 6) nuclei/20× field were found within MyHC^{+} cell bodies. In myoblast preparations from *Pax7*$^{lacZ/lacZ}$ muscle, an average of 3.0 ± 1.5 (n = 11) nuclei were found within MyHC^{+} cell bodies. In myoblast preparations from *Pax7*$^{lacZ/lacZ}$ muscle, all MyoD^{+} cells expressed MyHC after 6 d of culture in differentiation conditions. In contrast, in the *Pax7*$^{+/lacZ}$ control, ~10% of MyoD^{+} cells did not express MyHC.

Lastly, EDL fiber bundles containing interstitial connective and other tissues from P30 *Pax7*$^{+/lacZ}$ and *Pax7*$^{lacZ/lacZ}$ mice were plated on Matrigel and cultured for 3 d in growth media followed by 1 d in differentiation media. *Pax7*$^{+/lacZ}$ EDL muscle yielded large numbers of MyoD-, Myf5-, and MyHC-expressing cells together with formation of large myotubes (Fig. 5 C). Notably, *Pax7*$^{lacZ/lacZ}$ EDL myofiber bundles gave rise to low numbers of MyoD- and Myf5-expressing cells that were capable of forming myotubes (Fig. 5 D). However, under identical conditions, *Pax7*$^{lacZ/lacZ}$ single fibers free of interstitial tissues did not yield any Myf5-, MyoD-, or MyHC-expressing cells (see Absence of functional satellite cells...). Together, these results indicate that a low number of *Pax7*$^{lacZ/lacZ}$ myogenic cells resides in an alternate anatomical location and support the contention that *Pax7*$^{lacZ/lacZ}$ myogenic cells represent an interstitial myogenic-progenitor population distinct from the satellite cell compartment.

Coexpression of Pax3 and myogenic markers in *Pax7*$^{lacZ/lacZ}$ cells

To investigate the possibility that the Pax7-independent myogenic cells in adult muscle represent a Pax3-dependent lineage, cell cultures from limb and diaphragm were analyzed for Pax3 expression by immunohistochemistry. Cultures from both wild-type and *Pax7*$^{lacZ/lacZ}$ diaphragm (unpublished data) and limb (Fig. 5 B) muscles yielded similar numbers of MyoD$^+$/Pax3$^+$ cells (Fig. 5 B). The majority of wild-type MyoD$^+$ cells did not express Pax3 (Fig. 5 B, arrows) but expressed Pax7 (not depicted). However, in cultures derived from *Pax7*$^{lacZ/lacZ}$ muscle, virtually all MyoD$^+$ cells coexpressed Pax3 (Fig. 5 B, arrowheads), with very few MyoD$^+$/Pax3$^-$ cells detected. Altogether, these results suggest that Pax3 is expressed in a population of myogenic progenitors in adult *Pax7*$^{lacZ/lacZ}$ muscle.

Pax3$^+$ myogenic cells in adult skeletal muscle

To demonstrate the presence of the Pax3$^+$ myogenic cell population in wild-type animals, we performed RNase protection assay, in situ hybridization, and immunostaining on wild-type muscles. By RNase protection assay, primary myoblasts isolated from adult limb muscles and expanded over several weeks expressed extremely low levels of *Pax3* mRNA, and we were unable to detect Pax3 protein by Western blot analysis (unpublished data). In addition, *Pax3* mRNA was below the limit of detection in C2C12 myoblasts and myotubes. Furthermore, immunolabeling for Pax3 confirmed the presence of Pax3-expressing cells in wild type and *Pax7*$^{lacZ/lacZ}$ limb musculature outside the basal lamina (Fig. 6, A–E and G–K). In contrast, Pax7$^+$ cells in *Pax7*$^{+/lacZ}$ muscle were uniformly observed in a sublaminar position (Fig. 6, B and E). Limb muscle of wild-type mice at P1 was also examined and we found a similar interstitial localization of Pax3$^+$ cells and sublaminar positioning of Pax7$^+$ cells (Fig. S2, available at http://www.jcb.org/cgi/content/full/jcb.200508001/DC1). In situ hybridization also detected the presence of Pax3-expressing cells within the musculature of both wild type and *Pax7*$^{lacZ/lacZ}$ diaphragm (Fig. 6, F and L). Immunolabeling of the basal lamina confirmed the location of the Pax3$^+$ cells outside the satellite cell location in the diaphragm (unpublished data). In agreement with the in vitro data, Pax3$^+$ cells were found at a similar abundance in both *Pax7*$^{lacZ/lacZ}$ and *Pax7*$^{+/+}$ muscle (1.6 ± 0.5 and 1.1 ± 0.5 Pax3$^+$ cells/section in *Pax7*$^{+/+}$ and *Pax7*$^{lacZ/lacZ}$ by in situ hybridization, respectively). These analyses reveal the presence of myogenic Pax3$^+$ cells in the interstitial environment in a niche distinct from the satellite cell compartment in both mutant and wild-type musculature.

Coexpression of Pax3 and MyoD during muscle regeneration in vivo

Finally, we tested for whether the rare Pax3$^+$ myogenic cells have any biological function in vivo. TA and gastrocnemius muscles were examined for expression of Pax3 and MyoD 2 d after CTX-induced regeneration. In resting muscles, none of the Pax3$^+$ cells expressed MyoD in either *Pax7*$^{+/lacZ}$ or *Pax7*$^{lacZ/lacZ}$ mice (Fig. 7 and not depicted). Within 2 d after CTX injection in *Pax7*$^{+/lacZ}$ mice, ~84% Pax3$^+$ cells expressed

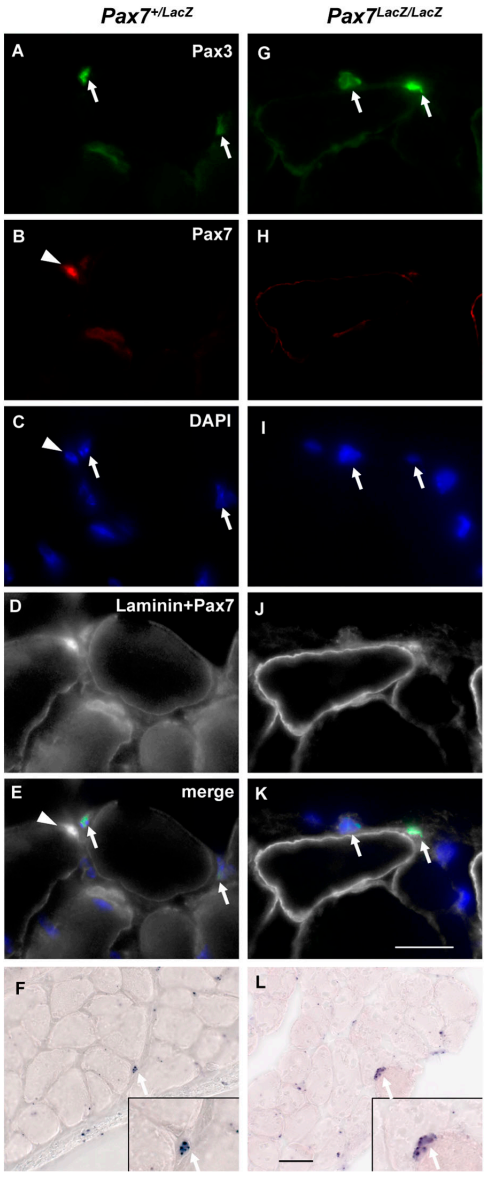

Figure 6. **Pax3 expression in *Pax7*$^{lacZ/lacZ}$ and *Pax7*$^{+/lacZ}$ musculature.** (A–E and G–K) Triple staining of adult EDL muscle sections with laminin, Pax7, and Pax3 antibodies plus DAPI labeling of nuclei. Pax3$^+$ cells (arrows), located in the interstitial space outside the basal lamina of myofibers, exist in similar frequency in both *Pax7*$^{+/lacZ}$ (C) and *Pax7*$^{lacZ/lacZ}$ (D) muscles. Note that the Pax7$^+$ cell (arrowheads) in the *Pax7*$^{+/lacZ}$ is located in a sublaminar position. Bar, 10 μm. (F and L) Pax3 in situ hybridization on *Pax7*$^{+/lacZ}$ (F) and *Pax7*$^{lacZ/lacZ}$ (L) diaphragm also revealed the presence of Pax3$^+$ cells in both genotypes. Bar, 25 μm.

MyoD (n = 74 cells from four 20× microscopic images taken from regenerative regions); ~11% of the MyoD$^+$ cells were also Pax3$^+$ (n = 569 cells from four regenerative regions; Fig. 7). In the regenerating muscles of *Pax7*$^{lacZ/lacZ}$ mice, ~29% Pax3$^+$ cells coexpressed MyoD (Fig. 7; n = 80 cells from five regenerating regions). Whereas the number of Pax3$^+$ cells was comparable in *Pax7*$^{+/lacZ}$ and *Pax7*$^{lacZ/lacZ}$ muscles, the total number of MyoD$^+$ cells in regenerating *Pax7*$^{lacZ/lacZ}$ muscle was only 5% of that in *Pax7*$^{+/lacZ}$ muscles, a result consistent with the impaired muscle regeneration in mutant mice. Among the

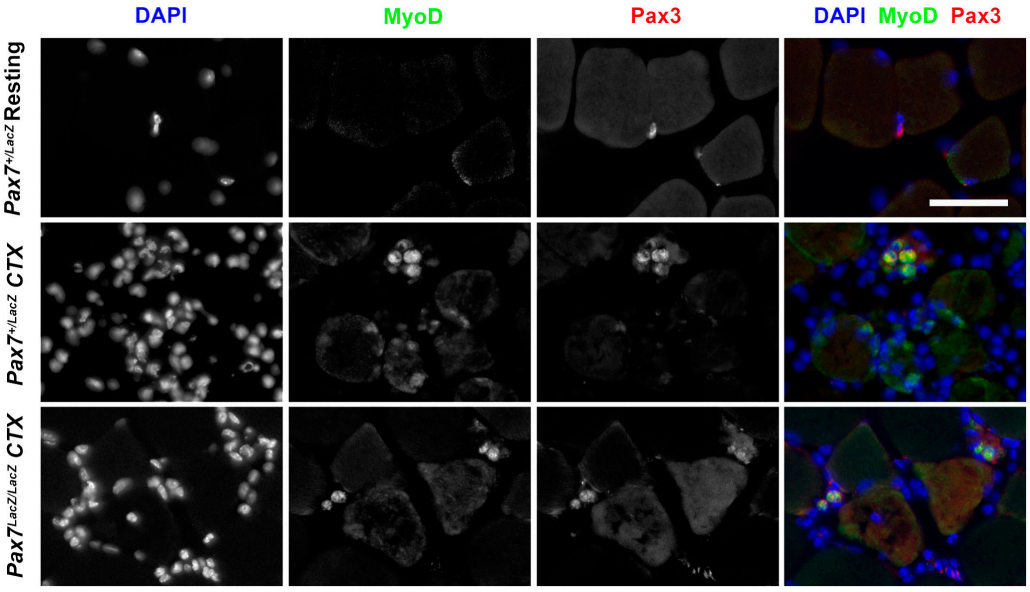

Figure 7. **Myogenic specification of Pax3$^+$ cells during muscle regeneration.** In resting muscle, Pax3$^+$ cells did not coexpress MyoD. In regenerating *Pax7*$^{lacZ/lacZ}$ and *Pax7*$^{+/lacZ}$ muscles 48 h after CTX injection, many Pax3$^+$ cells coexpressed MyoD, indicating that these cells had acquired a myogenic fate. Note that in *Pax7*$^{+/lacZ}$, the majority of MyoD$^+$ cells did not express Pax3 and are likely expressing Pax7. Bar, 20 μm.

MyoD$^+$ cells in *Pax7*$^{lacZ/lacZ}$ regenerating muscles (n = 38 cells from five regenerative regions), ~61% coexpressed Pax3, suggesting that the majority of MyoD$^+$ cells were derived from the Pax3 myogenic cells. In addition, the frequency of Pax3$^+$ cells in the regenerating region (>10 cells/field) was higher than in the resting tissue (1–2 cells/section; see the previous paragraph), suggesting that Pax3$^+$ myogenic cells are preferentially recruited to the regenerating region and/or Pax3 expression is upregulated during regeneration. Together, these results indicate that these interstitial Pax3$^+$ cells found in limb musculature likely represent a novel lineage of myogenic progenitors that is distinct from the Pax7$^+$ satellite cell lineage of myogenic cells.

Discussion

Our analysis of *Pax7*$^{lacZ/lacZ}$ mice clearly establishes an essential requirement for Pax7 during postnatal muscle growth and regeneration. Importantly, these experiments demonstrate that Pax7 is required for presatellite cells to express genes normally associated with functional satellite cells located in the sublaminar niche. Moreover, Pax7 is also required for the productive formation of committed myogenic precursor cells from sublaminar satellite cells. Furthermore, our experiments have identified a novel population of interstitial Pax3-expressing myogenic progenitors in adult limb musculature.

Using three different models of muscle injury in three different muscle groups, our results demonstrate a severe regeneration deficit in adult *Pax7*$^{lacZ/lacZ}$ mice. Profound deficits in *Pax7*$^{lacZ/lacZ}$ muscle regeneration have also been reported in a mixed C57/BL/Sv129 genetic background (Oustanina et al., 2004). Surprisingly, Oustanina et al. (2004) observed that postnatal muscle growth appeared "essentially normal" despite the extremely low number of satellite cells, the obviously smaller body size, and the increased number of smaller sized myofibers in *Pax7*$^{lacZ/lacZ}$ mice in the mixed background. Our experiments do not support these findings. We observed significant deficits in muscle growth and regeneration capacity in *Pax7*$^{lacZ/lacZ}$ mice with loss of fast myofibers, calcium deposition, and chronic degeneration associated with aging. The specific loss of fast muscle fibers can be attributed to the deficient fiber growth, as manifested by the reduced fiber size and myonuclei number per fiber, susceptibility of fast fibers to damages, and inefficient regeneration mechanisms to replace damaged fibers. In response to acute damage, such as CTX- or crush-induced injury, *Pax7*$^{lacZ/lacZ}$ muscle was rapidly replaced by an inflammatory infiltration, together with large calcium deposits and extensive adipose infiltration. Only rare regenerated myofibers were formed. Lastly, our results demonstrate that Pax7 is required for the normal function of satellite cells and the productive formation of myogenic precursor cells. Therefore, our study unequivocally demonstrates that *Pax7*-dependent myogenic cells, which comprise the satellite cell compartment, are required for the efficient regeneration of skeletal muscle.

The identification of rare regenerated *Pax7*$^{lacZ/lacZ}$ myofibers suggested the presence of Pax7-independent myogenic progenitors within the muscle. In our experiments, myogenic (MyoD$^+$) cells were cultured from *Pax7*$^{lacZ/lacZ}$ muscle at a frequency of ~1/150 as compared with wild-type muscle. However, our in vivo data suggests that Pax3$^+$ myogenic progenitors may give rise to as much as 5% of MyoD$^+$ cells during regeneration. Importantly, sufficient numbers of *Pax7*$^{lacZ/lacZ}$ myofibers were analyzed to conclusively demonstrate that these *Pax7*$^{lacZ/lacZ}$ myogenic cells were not associated with myofibers and therefore were not satellite cells. Specifically, control EDL myofibers contained ~9–10 Syndecan4$^+$ satellite cells per fiber. Therefore, if satellite cells were present on

Pax7$^{lacZ/lacZ}$ fibers at a frequency of 1/150, one satellite cell would be observed for every 16 fibers. From our experiments, no Syndecan4$^+$ cells were detected on a total of 197 fibers examined either by direct immunohistochemistry or following in vitro culture. Although few β-gal$^+$ cells (7% of control) were found on *Pax7*$^{lacZ/lacZ}$ fibers, these cells did not express the satellite cell markers CD34 and Syndecan4 and were incapable of on-fiber proliferation in culture, suggesting that they were incapable of productively forming myogenic precursor cells. In addition, single fiber versus myofiber bundle culture experiments strongly support the notion that the myogenic progenitors found in *Pax7*$^{lacZ/lacZ}$ mice were not associated with myofibers, arguing against a possible contribution from any residual Pax7-deficient satellite cells.

Recent findings have demonstrated the presence of resident or circulating stem cells in the muscle (Ferrari et al., 1998; Bittner et al., 1999; Gussoni et al., 1999; Blau et al., 2001; Torrente et al., 2001; Asakura et al., 2002; LaBarge and Blau, 2002; Qu-Petersen et al., 2002; Polesskaya et al., 2003; Dreyfus et al., 2004). Our results suggest that these stem cells are insufficient to compensate for the loss of satellite cell function in the absence of Pax7 or suggest that Pax7 is a key player in the myogenic specification of most, if not all, adult stem cells. This idea is further supported by our finding that the myogenic differentiation of Pax3$^+$ cells is reduced in the *Pax7*$^{lacZ/lacZ}$ mice, by our previous studies showing that Pax7 expression is necessary for the myogenic differentiation of CD45$^+$ muscle-derived stem cells (Seale et al., 2004), and by recent studies showing that embryonic stem cells giving rise to satellite cells apoptose or undergo nonmyogenic differentiation in the absence of Pax7 and -3 (Relaix et al., 2005).

The molecular function of Pax3 and -7 in myogenic specification remains to be fully defined. Genetically, *Pax3* and *-7* function upstream of *Myf5* and *MyoD*, and Pax3-FKHD is capable of activating MyoD transcription in fibroblasts (Khan et al., 1999). In addition, several recent studies have reported that newly activated satellite cells and proliferating myoblasts coexpress Pax7 and MyoD in vitro (Halevy et al., 2004; Olguin and Olwin, 2004; Zammit et al., 2004). Together, these findings support the notion that Pax3/Pax7 directly or indirectly activates the transcription of the myogenic regulatory factors. Moreover, ectopic expression of Pax7 leads to enhanced proliferative and survival potential of myoblasts (Seale et al., 2004). Likewise, transient activation of Pax3 expression in response to Notch signaling has been reported in cultures of primary myoblast (Conboy and Rando, 2002), resulting in enhanced proliferation of these cells. Interestingly, overexpression of Pax7 also seems to down-regulate MyoD and promote cell-cycle withdrawal from the proliferating state, therefore playing a critical role in the maintenances of the satellite cell pool (Olguin and Olwin, 2004; Zammit et al., 2004). Our present data demonstrate that satellite cells lacking Pax7 undergo arrest when forming myogenic cells. Pax7 appears to function at multiple levels, including activation of the myogenic program, stimulating the proliferation and survival of myogenic progenitors, and the self-renewal of satellite cells. Our experiments unequivocally demonstrate that Pax7-deficient satellite cells that survive are incapable of giving rise to functional myogenic progenitors. Therefore, we conclude that Pax7 is required for sublaminar satellite cells to either form functional myogenic daughter cells or maintain a renewable satellite cell pool. Importantly, these data imply that myogenic commitment or specification occurs when satellite cells undergo an asymmetric cell division to form a myogenic factor–expressing daughter cell.

The rare MyoD$^+$ cells recovered from whole muscle homogenates from *Pax7*$^{lacZ/lacZ}$ mice uniformly expressed Pax3. Immunolabeling and in situ hybridization revealed the presence of Pax3$^+$ cells in interstitial locations outside the basal lamina of muscle fibers and not in the sublaminar satellite cell niche. The interstitial Pax3$^+$ cells did not express MyoD in undamaged muscle. However, after injury, the Pax3$^+$ cells rapidly increased in number and were found to express MyoD. Expression of *Pax3-GFP* or *Pax3-nLacZ* knockins has recently been reported in postnatal diaphragm in a subset of Pax7-expressing satellite cells, but expression was not detected in satellite cells in most hind limb musculature (Buckingham et al., 2003; Montarras et al., 2005; Relaix et al., 2005), as opposed to our observation that they are located outside muscle fibers. In our experiments, we only detected Pax3 protein in rare cells located outside of the basal lamina and not in satellite cells. This discrepancy may be the result of the different labeling techniques used and the different thresholds of detection between immunostaining of endogenous Pax3 versus bacterial enzymes or GFP with long half-lives. It is also possible that the extralaminar Pax3-expressing cells represent presatellite cells that require Pax7 to become functional sublaminar satellite cells. However, the presence of these cells in both wild type and mutant muscle, and the absence of detectable Pax3 protein in Pax7-deficient LacZ$^+$ cells, supports the notion that the Pax3$^+$ cells represent a novel myogenic lineage. Future studies applying immunolabeling to the knockin mice may help clarify the discrepancy.

Together, our experiments suggest that the interstitial Pax3$^+$ cells represent a novel myogenic lineage that is distinct from the sublaminar Pax7$^+$ satellite cell compartment. The normal role of these Pax3-expressing myogenic progenitors in adult muscle remains to be established. It is interesting to speculate that Pax3-expressing myogenic cells have a specialized role in adult muscle. For example, it is possible that these cells have a role in the formation of muscle spindles, neuromuscular junctions, myotendinous attachments, or other muscle specializations. Future studies characterizing the expression, differential activity, and developmental role of Pax3 and -7 in postnatal myogenesis are thus required.

Materials and methods

Mice and injury protocols

Mice carrying a targeted reporter allele of *Pax7* provided by P. Gruss (Max Plank Institute for Biophysical Chemistry, Göttingen, Germany; Mansouri et al., 1996) were backcrossed into the 129Sv/J genetic background for nine generations to generate 129Sv/J-inbred mice carrying the *Pax7-LacZ* allele. In these mice, the *Pax7* gene was knocked out by insertion of a β-gal gene and a neomycin cassette into the first exon of *Pax7*. The muscle phenotype was indistinguishable between C57BL/6- or 129Sv/J-inbred backgrounds and a C57BL/6 × 129Sv/J-outbred background. Mouse serum was prepared by coagulation and centrifugation of

blood samples and assayed by the Department of Biochemistry at the Children Hospital of Eastern Ontario. To investigate whether regeneration is age dependent, 1–7-mo-old *Pax7*$^{lacZ/lacZ}$ and *Pax7*$^{+/+}$ littermates were used for all regeneration experiments. However, no difference was found in the regeneration efficiency of age groups tested. We therefore pooled all data together in the results. For CTX-induced muscle regeneration, mice were killed at 10 d or 1 mo after injection of 25 μl CTX (10 μM; Latoxan) into the TA or the gastrocnemius muscles. For cell proliferation assays, 30 mg/kg BrdU (Sigma-Aldrich) was injected i.p. on days 4, 6, 7, and 8 after CTX injection. For crush injury, TA or gastrocnemius muscles were crushed using large forceps. Experiments were performed under University of Ottawa regulations for animal care and handlings.

Cell and tissue culture

Single myofibers were isolated by collagenase digestion as previously described (Charge et al., 2002) and subsequently plated in Matrigel-coated chamber slides for attached culture or suspended in 60-mm Petri dishes coated with horse serum to prevent fiber attachment. Myofiber bundles, which contained ~10–50 myofibers and surrounding tissue, were prepared and plated in chamber slides as per single myofiber culture but without extensive trituration. Primary myoblasts were isolated from hind limb or diaphragm muscles and cultured as previously described (Megeney et al., 1996).

Histology

For all injury and regeneration experiments, TA muscle was isolated, cut at mid-belly, embedded in optimal cutting temperature compound (Tissue-Tek)/20% sucrose, and frozen in liquid nitrogen for cryosections or fixed in 4% PFA and processed for paraffin sections. Cryosections were used for immunohistochemistry staining, and paraffin sections were used for hematoxylin–eosin, Alizarin red S (calcification), or Van Gieson's (fibrosis) staining. For postnatal fiber size analysis, lower hind legs were cryosectioned and total fiber number and fiber size were analyzed on transverse sections (10 μm) of the mid-belly soleus and EDL muscles, using NIH Image software. Fiber types were identified immunohistochemically with antibodies specific for MyHC subtypes (see next section) as described previously (Hughes et al., 1993).

Immunochemistry

In brief, cryosections, single myofibers, or cultured cells were fixed in 2–4% PFA, quenched with glycine (100 mM glycine, 0.2% Triton X-100, and 0.1% sodium azide in PBS), and blocked in PBS containing 2% BSA, 5% goat serum, and 0.2% Triton X-100. Tissues or cells were then incubated with the primary antibodies diluted in the same blocking solution and finally with biotinylated secondary antibodies or fluorophore-conjugated secondary antibodies. The primary antibodies used were as follows: mouse monoclonal anti-Pax3 (IgG2a; a gift from C. Ordhal, University of California, San Francisco, San Francisco, CA; available from the Developmental Studies Hybridoma Bank), rabbit anti-Pax3 (Active Motif and Zymed Laboratories), Pax7 (Developmental Studies Hybridoma Bank), rat anti-laminin (Qbiogene), laminin (DakoCytomation), Desmin (DakoCytomation), CD34 (BD Biosciences), MyoD (5.8A; BD Biosciences), rabbit anti-MyoD (C-20; Santa Cruz Biotechnology, Inc.), Myf5 (Santa-Cruz Biotechnology, Inc.), MyHC (MF-20; Developmental Studies Hybridoma Bank), embryonic fast MyHC (F1.652; Developmental Studies Hybridoma Bank); MyHC IIb (BF-F3; Deutsche Sammlung von Mikroorganismen und Zellkulturen), MyHC I (A4.840) and IIa (A4.74; Developmental Studies Hybridoma Bank), anti–β-gal (Invitrogen), and chicken anti-Syndecan4 (gift of B. Olwin, University of Colorado, Boulder, CO; Cornelison et al., 2001). BrdU detection was performed using the BrdU in situ detection kit (BD Biosciences) following the manufacturer's protocol. The secondary antibodies used were Alexa488 anti-mouse IgG2a; Alexa568 anti-mouse IgG1 (Invitrogen); and Fluorescein-, Rhodamine-, or Cy5-conjugated antibodies (Chemicon). Nuclei were counter-stained with DAPI.

In situ hybridization

Pax7$^{+/+}$ and *Pax7*$^{lacZ/lacZ}$ adult diaphragms were processed for in situ hybridization as previously described (Wallace and Raff, 1999). A *Pax3* cDNA template was used for synthesis of sense and antisense digoxigenin-labeled riboprobes (Goulding et al., 1993). After in situ hybridization, sections were reacted with an antibody to laminin (DakoCytomation) and a Rhodamine-conjugated secondary layer (Chemicon).

Statistical analysis and microscopy

Errors quoted are SEM throughout. Data were analyzed using unpaired *t* tests. Asterisks indicate significance at $P < 0.05$ and $P < 0.01$ throughout. Samples were visualized with a microscope (Axioplan2; Carl Zeiss MicroImaging, Inc.), and images were acquired using a camera (AxioCam; Carl Zeiss MicroImaging, Inc.) and the Axioview 3.1 software (Carl Zeiss MicroImaging, Inc.). Digital fluorescent images were captured at room temperature with a 20× (plan-apochromat, air, NA 0.75) or 63× (plan-apochromat, oil, NA 1.40) objective using the least possible exposure to minimize bleaching. The final displaying levels were subsequently adjusted similarly for all figures using Axioview or Photoshop (Adobe) software.

Online supplemental material

Fig. S1 shows the expression of β-gal in *Pax7*$^{+/lacZ}$ and *Pax7*$^{lacZ/lacZ}$ muscles at P0. Fig. S2 shows Pax7^{+} and Pax3^{+} cells in the limb muscle of a wild-type mouse at P1. Online supplemental material is available at http://www.jcb.org/cgi/content/full/jcb.200508001/DC1.

We thank Dr. B. Olwin for the gift of Syndecan4 antibody and Vanessa Seale for technical assistance.

S. Kuang was supported by a postdoctoral fellowship from the National Sciences and Engineering Research Council. P. Seale was supported by a doctoral research award from the Canada Institutes of Health Research. M.A. Rudnicki holds the Canada Research Chair in Molecular Genetics and is a Howard Hughes Medical Institute International Scholar. This work was supported by grants to M.A. Rudnicki from the Muscular Dystrophy Association, the National Institutes of Health, the Canada Institutes of Health Research, and the Canada Research Chair Program.

Submitted: 1 August 2005
Accepted: 6 December 2005

References

Asakura, A., P. Seale, A. Girgis-Gabardo, and M.A. Rudnicki. 2002. Myogenic specification of side population cells in skeletal muscle. *J. Cell Biol.* 159:123–134.

Beauchamp, J.R., L. Heslop, D.S. Yu, S. Tajbakhsh, R.G. Kelly, A. Wernig, M.E. Buckingham, T.A. Partridge, and P.S. Zammit. 2000. Expression of CD34 and Myf5 defines the majority of quiescent adult skeletal muscle satellite cells. *J. Cell Biol.* 151:1221–1234.

Ben-Yair, R., and C. Kalcheim. 2005. Lineage analysis of the avian dermomyotome sheet reveals the existence of single cells with both dermal and muscle progenitor fates. *Development.* 132:689–701.

Bittner, R.E., C. Schofer, K. Weipoltshammer, S. Ivanova, B. Streubel, E. Hauser, M. Freilinger, H. Hoger, A. Elbe-Burger, and F. Wachtler. 1999. Recruitment of bone-marrow-derived cells by skeletal and cardiac muscle in adult dystrophic mdx mice. *Anat. Embryol. (Berl.).* 199:391–396.

Blau, H.M., T.R. Brazelton, and J.M. Weimann. 2001. The evolving concept review of a stem cell: entity or function? *Cell.* 105:829–841.

Bober, E., T. Franz, H.H. Arnold, P. Gruss, and P. Tremblay. 1994. Pax-3 is required for the development of limb muscles: a possible role for the migration of dermomyotomal muscle progenitor cells. *Development.* 120:603–612.

Buckingham, M., L. Bajard, T. Chang, P. Daubas, J. Hadchouel, S. Meilhac, D. Montarras, D. Rocancourt, and F. Relaix. 2003. The formation of skeletal muscle: from somite to limb. *J. Anat.* 202:59–68.

Charge, S.B., and M.A. Rudnicki. 2004. Cellular and molecular regulation of muscle regeneration. *Physiol. Rev.* 84:209–238.

Charge, S.B., A.S. Brack, and S.M. Hughes. 2002. Aging-related satellite cell differentiation defect occurs prematurely after Ski-induced muscle hypertrophy. *Am. J. Physiol. Cell Physiol.* 283:C1228–C1241.

Conboy, I.M., and T.A. Rando. 2002. The regulation of Notch signaling controls satellite cell activation and cell fate determination in postnatal myogenesis. *Dev. Cell.* 3:397–409.

Cornelison, D.D., M.S. Filla, H.M. Stanley, A.C. Rapraeger, and B.B. Olwin. 2001. Syndecan-3 and syndecan-4 specifically mark skeletal muscle satellite cells and are implicated in satellite cell maintenance and muscle regeneration. *Dev. Biol.* 239:79–94.

Dreyfus, P.A., F. Chretien, B. Chazaud, Y. Kirova, P. Caramelle, L. Garcia, G. Butler-Browne, and R.K. Gherardi. 2004. Adult bone marrow-derived stem cells in muscle connective tissue and satellite cell niches. *Am. J. Pathol.* 164:773–779.

Ferrari, G., G. Cussela-De Angelis, M. Coletta, E. Paolucci, A. Stornaiuolo, G. Cossu, and F. Mavilio. 1998. Muscle regeneration by bone marrow-derived myogenic progenitors. *Science.* 279:1528–1530.

Goulding, M., S. Sterrer, J. Fleming, R. Balling, J. Nadeau, K.J. Moore, S.D. Brown, K.P. Steel, and P. Gruss. 1993. Analysis of the Pax-3 gene in the mouse mutant splotch. *Genomics.* 17:355–363.

Goulding, M., A. Lumsden, and A.J. Paquette. 1994. Regulation of Pax-3 expression in the dermomyotome and its role in muscle development. *Development.* 120:957–971.

Gros, J., M. Manceau, V. Thome, and C. Marcelle. 2005. A common somitic origin for embryonic muscle progenitors and satellite cells. *Nature.* 435:954–958.

Gussoni, E., Y. Soneoka, C.D. Strickland, E.A. Buzney, M.K. Khan, A.F. Flint, L.M. Kunkel, and R.C. Mulligan. 1999. Dystrophin expression in the mdx mouse restored by stem cell transplantation. *Nature.* 401:390–394.

Halevy, O., Y. Piestun, M.Z. Allouh, B.W. Rosser, Y. Rinkevich, R. Reshef, I. Rozenboim, M. Wleklinski-Lee, and Z. Yablonka-Reuveni. 2004. Pattern of Pax7 expression during myogenesis in the posthatch chicken establishes a model for satellite cell differentiation and renewal. *Dev. Dyn.* 231:489–502.

Hughes, S.M., M. Cho, I. Karsch-Mizrachi, M. Travis, L. Silberstein, L.A. Leinwand, and H.M. Blau. 1993. Three slow myosin heavy chains sequentially expressed in developing mammalian skeletal muscle. *Dev. Biol.* 158:183–199.

Kassar-Duchossoy, L., E. Giacone, B. Gayraud-Morel, A. Jory, D. Gomes, and S. Tajbakhsh. 2005. Pax3/Pax7 mark a novel population of primitive myogenic cells during development. *Genes Dev.* 19:1426–1431.

Khan, J., M.L. Bittner, L.H. Saal, U. Teichmann, D.O. Azorsa, G.C. Goooden, W.J. Pavan, J.M. Trent, and P.S. Meltzer. 1999. cDNA microarrays detect activation of a myogenic transcription program by the PAX3-FKHR fusion oncogene. *Proc. Natl. Acad. Sci. USA.* 96:13264–13269.

LaBarge, M.A., and H.M. Blau. 2002. Biological progression from adult bone marrow to mononucleate muscle stem cell to multinucleate muscle fiber in response to injury. *Cell.* 111:589–601.

Mansouri, A., A. Stoykova, M. Torres, and P. Gruss. 1996. Dysgenesis of cephalic neural crest derivatives in *Pax7*$^{-/-}$ mutant mice. *Development.* 122:831–838.

Megeney, L.A., B. Kablar, K. Garrett, J.E. Anderson, and M.A. Rudnicki. 1996. MyoD is required for myogenic stem cell function in adult skeletal muscle. *Genes Dev.* 10:1173–1183.

Montarras, D., J. Morgan, C. Collins, F. Relaix, S. Zaffran, A. Cumano, T. Partridge, and M. Buckingham. 2005. Direct isolation of satellite cells for skeletal muscle regeneration. *Science.* 309:2064–2067.

Olguin, H.C., and B.B. Olwin. 2004. Pax-7 up-regulation inhibits myogenesis and cell cycle progression in satellite cells: a potential mechanism for self-renewal. *Dev. Biol.* 275:375–388.

Oustanina, S., G. Hause, and T. Braun. 2004. Pax7 directs postnatal renewal and propagation of myogenic satellite cells but not their specification. *EMBO J.* 23:3430–3439.

Parker, M.H., P. Seale, and M.A. Rudnicki. 2003. Looking back to the embryo: transcriptional networks in adult myogenesis. *Nat Rev. Genet.* 4:497–507.

Polesskaya, A., P. Seale, and M.A. Rudnicki. 2003. Wnt signaling induces the myogenic specification of resident CD45+ adult stem cells during muscle regeneration. *Cell.* 113:841–852.

Qu-Petersen, Z., B. Deasy, R. Jankowski, M. Ikezawa, J. Cummins, R. Pruchnic, J. Mytinger, B. Cao, C. Gates, A. Wernig, and J. Huard. 2002. Identification of a novel population of muscle stem cells in mice: potential for muscle regeneration. *J. Cell Biol.* 157:851–864.

Relaix, F., D. Rocancourt, A. Mansouri, and M. Buckingham. 2004. Divergent functions of murine Pax3 and Pax7 in limb muscle development. *Genes Dev.* 18:1088–1105.

Relaix, F., D. Rocancourt, A. Mansouri, and M. Buckingham. 2005. A Pax3/Pax7-dependent population of skeletal muscle progenitor cells. *Nature.* 435:948–953.

Seale, P., L.A. Sabourin, A. Girgis-Gabardo, A. Mansouri, P. Gruss, and M.A. Rudnicki. 2000. Pax7 is required for the specification of myogenic satellite cells. *Cell.* 102:777–786.

Seale, P., J. Ishibashi, A. Scime, and M.A. Rudnicki. 2004. Pax7 is necessary and sufficient for the myogenic specification of CD45^{+}:Sca1^{+} stem cells from injured muscle. *PLoS Biol.* 2:E130.

Tajbakhsh, S., D. Rocancourt, G. Cossu, and M. Buckingham. 1997. Redefining the genetic hierarchies controlling skeletal myogenesis: Pax-3 and Myf-5 act upstream of MyoD. *Cell.* 89:127–138.

Torrente, Y., J.P. Tremblay, F. Pisati, M. Belicchi, B. Rossi, M. Sironi, F. Fortunato, M. El Fahime, M.G. D'Angelo, N.J. Caron, et al. 2001. Intraarterial injection of muscle-derived CD34^{+}Sca-1^{+} stem cells restores dystrophin in *mdx* mice. *J. Cell Biol.* 152:335–348.

Wallace, V.A., and M.C. Raff. 1999. A role for Sonic hedgehog in axon-to-astrocyte signalling in the rodent optic nerve. *Development.* 126:2901–2909.

Zammit, P.S., J.P. Golding, Y. Nagata, V. Hudon, T.A. Partridge, and J.R. Beauchamp. 2004. Muscle satellite cells adopt divergent fates: a mechanism for self-renewal? *J. Cell Biol.* 166:347–357.